

Palladium minerals from the Cauê iron mine, Itabira District, Minas Gerais, Brazil

GEMA RIBEIRO OLIVO AND MICHEL GAUTHIER

Université du Québec à Montréal, Département des sciences de la terre, case postale 8888, succ. A, Montréal, PQ, Canada, H3C 3P8

Abstract

Palladium-bearing minerals from the Cauê iron mine, Itabira District, Minas Gerais, Brazil, are found in gold-rich jacutinga, a hydrothermally-altered Lake Superior-type carbonate-bearing oxide facies iron-formation. Palladium occurs as: native palladium with trace contents of Au, Fe and Cu; palladseite ((Pd,Cu,Hg)₁₇Se₁₅), which was found in the core of a grain of palladium; palladium-copper oxide ((Pd,Cu)O); and arsenopalladinite (Pd₈(As,Sb)₃), with inclusions of palladium-copper oxide. The palladium and palladium-copper oxide grains are coated with films of gold and commonly do not exceed 100 µm in width. These palladium minerals occur in hematite bands and in boudinaged bands of quartz and white phyllosilicate parallel to the S1 mylonitic foliation. Palladium-copper oxide also occurs as inclusions in gold grains which are strongly to weakly stretched parallel to S1.

Palladium mineralization is interpreted as synchronous with intense D1 shearing and contemporaneous with the peak of thermal metamorphism. At high oxygen fugacities and high temperatures (up to 600°C), Pd may have been transported as chloride complexes and deposited following changes in pH caused by mineralizing fluids reacting with jacutinga. Deposition may also have been prompted by the formation of insoluble selenide and arsenide-antimonide minerals and by the dilution of Cl concentrations in the mineralizing fluid. Textural studies, and the zonation observed in palladium and other hydrothermal minerals, suggest that oscillations in the physico-chemical conditions of hydrothermal fluids occurred during the mineralizing event.

KEYWORDS: palladium minerals, palladseite, arsenopalladinite, Cauê mine, Brazil, jacutinga.

Introduction

PALLADIUM minerals in the Itabira region were first described by Clark *et al.* (1974). These minerals were recovered from 4 g of residual concentrates from the gold washing in Itabira and consist of various quantities of three palladium arsenide-antimonides. The principal phase is arsenopalladinite (Pd₅(As,Sb)₂), later recalculated to Pd₈(As,Sb)₃ by Cabri *et al.* (1977), followed by minor quantities of isomertieite, (Pd,Cu)₅(Sb,As)₂, atheneite, (Pd,Hg)₃As, and a palladium selenide, identified as palladseite (Pd₁₇Se₁₅) (Davis *et al.*, 1977). Recently, Jedwab *et al.* (1993) reported the presence of palladium oxides (palladinite) in museum samples (rocks and concentrates) from Itabira.

These previous studies described the crystallographic and mineralogical characteristics of the

minerals, but as most of them were found in concentrates, not in host-rock, textural features and a genetic interpretations were not provided. This is reviewed here, where textural details and analytical data for palladium minerals found in the primary palladium-bearing gold ore of the Cauê iron mine, Itabira District, Brazil, are reported and discussed in terms of their genesis.

Geological setting

The Cauê iron mine is situated in the northeastern part of the Itabira Iron District, in the southern Sao Francisco craton (Fig. 1). At the Cauê mine, four geologic units metamorphosed to amphibolite facies have been identified (Fig. 2, Olivo *et al.*, 1995). They are commonly correlated with units of the Quadrilátero Ferrífero, also in the southern Sao

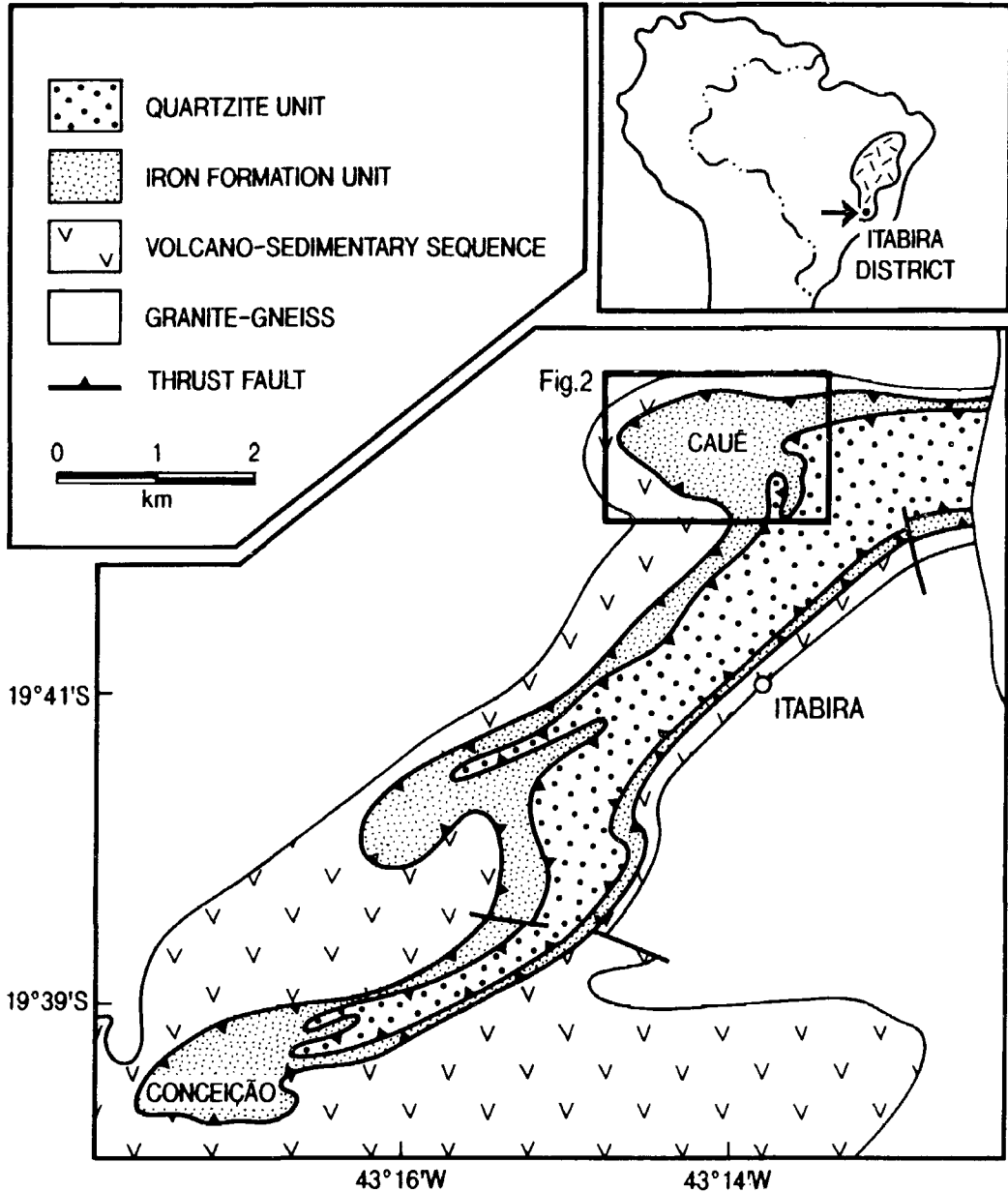


FIG. 1. Simplified map of the Itabira District (after Olivo *et al.*, 1995).

Francisco Craton. The four geologic units are, from the bottom to the top: (1) a volcano-sedimentary sequence correlated with the Archaean Rio das Velhas Supergroup; (2) a Lake Superior-type iron-formation unit composed of itabirite (e.g. metamorphosed banded siliceous ironstone consisting of interlayered

quartz-hematite-magnetite), massive hematite and jacutinga (e.g. hydrothermally altered carbonate-bearing oxide facies iron-formation, hosting gold and palladium mineralization) which is part of the Early Proterozoic, Lake Superior-type iron formation of the Itabira Group, Minas Gerais Supergroup; (3) a

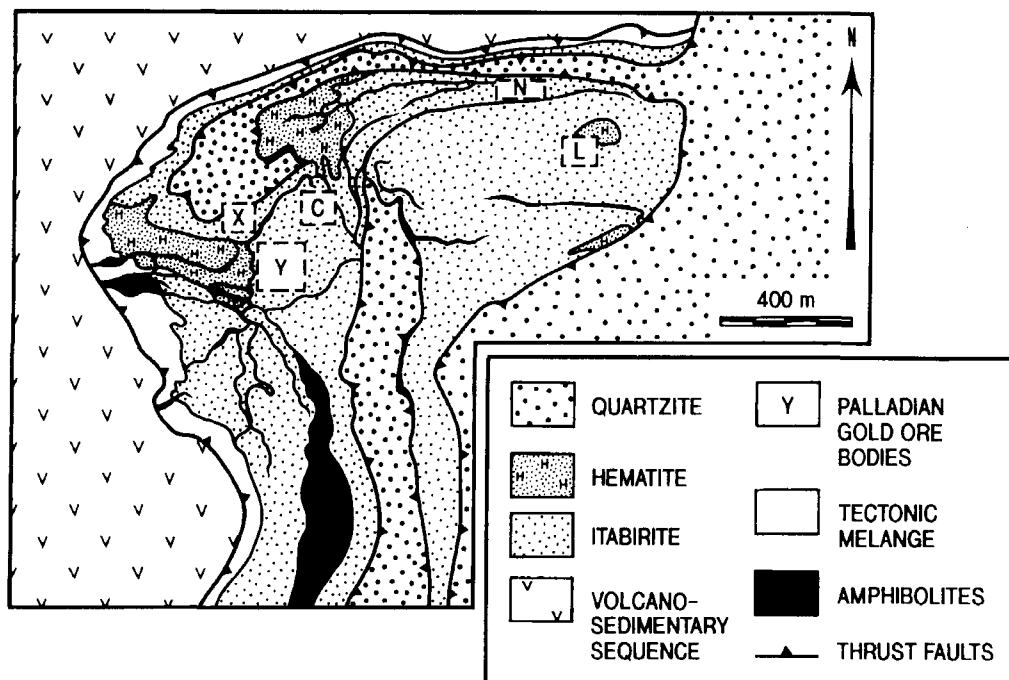


FIG. 2. Simplified geologic map of the Cauê iron mine, Itabira District, Minas Gerais State, Brazil, showing the palladian gold orebodies (C= Central; L= Aba Leste; N= Aba Norte; X= Corpo X; Y= Corpo Y). Modified after Leao de Sá and Borges (1991).

quartzite unit, correlated with the Early Proterozoic Piracicaba Group, Minas Supergroup; and (4) Archaean tectonic slices and Proterozoic dykes of mafic intrusive rocks (amphibolites).

These rocks were affected by three phases of folding, boudinage and thrust faulting (Olivo *et al.*, 1995). The D1-structures are tight to isoclinal folds becoming sheath folds where the ENE elongation lineation (Le) and mylonitic foliation (S1) are well developed. The S1-foliation is contemporaneous with the peak of thermal metamorphism (Hoefs *et al.*, 1982). The D2-structures also include tight folds, associated parasitic fold axes and the S2 transposition foliation. The D3 structures are characterized by open folds and are associated with a crenulation cleavage.

Millimetric to decametric boudins occur in S1 and S2 foliation planes. Reverse and thrust faulting created imbricated sheets that are interpreted as synchronous with Proterozoic D1 deformation (Olivo *et al.*, in press). Reactivation of these faults occurred during D2 and D3 deformation events.

Electron-microscope (EMP) and scanning electron microscope (SEM) analytical techniques

Analyses were carried out using the Cameca Camebax and JEOL JXA-8900L automated wavelength-dispersive electron-microprobe (EMP) at McGill University. Calibration for the analyses was done using pure metals, except mercury for which the synthetic standard Cabri-451 (Pd_3HgTe_3) was used at 20 kV and 15 kV and 20 nA. The analytical precision is better than 2%. The presence of oxygen was estimated using hematite and cassiterite standards and energy dispersive spectrometry analysis.

Textural and compositional studies were undertaken with the Hitachi S-2300 scanning electron microscope (SEM), using a back-scattered-electron detector and energy-dispersive spectrometry (EDS) at the Université du Québec à Montréal. Elemental abundances stated here are all in weight percent, and the microprobe standards and polished sections were freshly polished before analysis.

TABLE 1. Wavelength-dispersive system analyses by electron-microprobe of palladium and palladseite, shown in Figs. 3 and 4, from jacutinga of the Corpo Y orebody. Data reported by Davis *et al.* (1977) and an average of 4 analyses obtained by energy-dispersive system analyses (*, with 0.15% Mn) are given for comparison

	Palladium	Palladseite	Palladseite	Palladseite*	Palladseite Davis <i>et al.</i> (1977)
Pd	91.99	54.50	55.70	60.03	55.77
Cu	1.31	2.95	3.08	2.45	3.99
Hg	n.d.	3.02	3.08	3.78	1.66
Se	n.d.	36.95	34.19	33.60	38.59
Au	1.98	0.08	0.06	n.d.	n.d.
Fe	1.31	0.48	0.66	n.d.	n.d.
Total	96.65	97.98	96.77	99.85	100.01

Palladium minerals: occurrences and chemical compositions

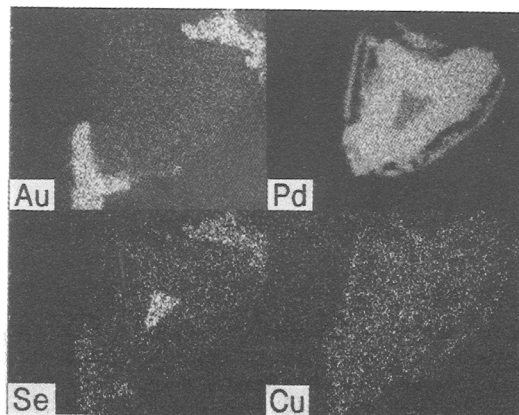
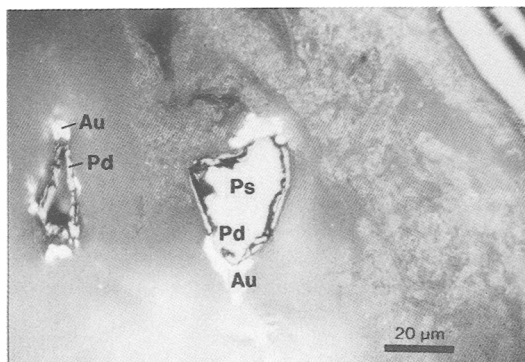
In the Cauê iron mine, gold and palladium have been mined as by-products in five orebodies (Fig. 2; Corpo Y, Corpo X, Central, Aba Leste, and Aba Norte; Olivo *et al.*, 1995) hosted by jacutinga. Palladium-bearing high-grade gold ores (up to 1000 g/t Au and 20 g/t Pd, L. Andrade, pers. comm.) are hosted by quartz- and hematite-rich bands parallel to the S1 mylonitic foliation and/or stretched parallel to the ENE elongation lineation.

Palladium-bearing minerals are observed in polished sections and in gravimetric concentrates of gold-rich jacutinga from the Corpo Y orebody. In this orebody, jacutinga comprises millimetric to centimetric bands of various concentrations of quartz (\pm feldspar), hematite (\pm goethite) and white

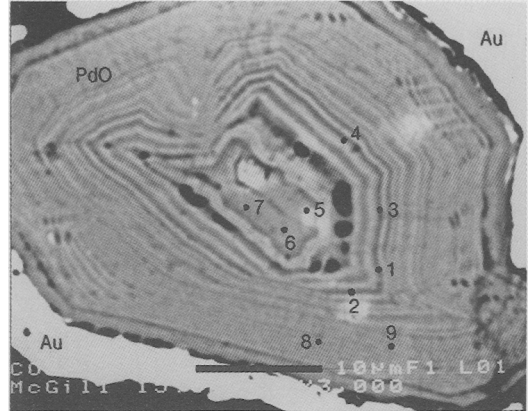
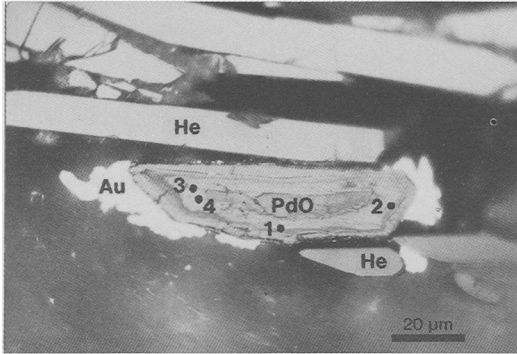
phyllo-silicates (talc \pm phlogopite \pm kaolin), with minor amounts of zoned tourmaline and monazite. Ankerite is common as inclusions in quartz grains. The palladium minerals occur in gold-rich bands parallel to the S1-foliation.

Palladium and palladseite. Four palladium grains occur in quartz and white phyllosilicate-rich boudins (Fig. 3) parallel to the S1 mylonitic foliation. These grains do not exceed 100 μ m, and are commonly coated with films of gold. In plane polarized light, palladium is creamy yellow in air and very light grey in oil immersion and is isotropic. Unfortunately, it does not polish well. The best analysis obtained for palladium is reported in Table 1, revealing that it is alloyed with small quantities of Au, Cu and Fe (< 2%).

One grain of palladium in a white phyllosilicate boudin has a core of palladseite (Table 1, Figs. 3



FIGS. 3 and 4. FIG. 3 (left). Photomicrograph of two palladium grains (Pd) coated with gold (Au) in a phyllosilicate-rich boudin parallel to S1; The large grain has a core of palladseite (Ps), and in the small grain, only the rim is preserved. FIG. 4 (right). Single-element scans of Pd, Cu, Au, and Se for the large palladium grain of Fig. 3 showing a core of palladseite.



FIGS 5 and 6. FIG. 5 (left). Photomicrograph of palladium-copper oxide (PdO) coated with gold (Au) in a hematite (He) band parallel to the S1 mylonitic foliation and stretched parallel to the elongation lineation. Zoning is characterized by the alternation of dark colored zones (high Pd/Cu ratios) with light zones (low Pd/Cu ratios). Arabic numbers correspond to analysed points referred to in Table 2. FIG. 6 (right). Back-scattered electron image showing finely zoned palladium-copper oxide (PdO) coated with gold occurring in white phyllosilicate band parallel to the S1 mylonitic foliation. Arabic numbers correspond to analysed points referred to in Table 2.

and 4) which polishes well in comparison with palladium. Palladseite is whitish cream in air and light grey in oil and is isotropic. The EMP analyses of palladseite obtained in this study are shown in Table 1. In addition to trace amounts of Fe and Au, it has lower Se and Cu contents and higher Hg contents than the values reported by Davis *et al.* (1977).

Palladium-copper oxide. Nine palladium copper oxide samples occur in hematite bands as free grains, stretched parallel to the elongation lineation Le (Fig. 5) and in quartz and white phyllosilicate boudins (Figs. 6 and 7) parallel to the S1 foliation. In plane polarized light in air or oil immersion, the palladium-oxide grains are medium-to-dark grey (darker than hematite), slightly anisotropic and without internal reflections. They show the same optical properties described for palladinite (PdO, Jedwab *et al.*, 1993). The grains are euhedral, finely zoned, coated with films of gold, and commonly do not exceed 100 µm (Figs. 5 and 6). The grain shown in Fig. 5 has a wide gold coating in the pressure-shadow regions, and this coating is slightly stretched along the S1 foliation plane.

Zoning in these minerals is characterized by the alternation of dark coloured zones (high Pd/Cu ratios) with light areas (low Pd/Cu ratios). This variation is most evident in grains with relatively coarse zonation (see Fig. 5 and Table 2). In the grains observed in Figs. 5 and 6, the Hg contents are high in the cores (up to 1.42%) and diminish toward the edges of the grains where the Hg contents are < 0.1%. Selenium and Sb contents are low (< 0.1%) and vary independently of the band colour and position in the grain (core or rim). Some palladium-copper oxide

grains also contain fine inclusions of gold oblique to the compositional bands (Fig. 7).

Small inclusions of Pd-Cu oxide (< 20 µm) showing island-mainland and replacement (relict) textures (Fig. 8), as defined by Ineson (1989), were also observed in gold grains that are parallel to the S1 foliation and slightly to highly stretched parallel to the elongation lineation (Olivo *et al.*, 1994).

Arsenopalladinite. One grain of arsenopalladinite was recovered from a mechanically disaggregated jacutinga sample. This grain contains inclusions of palladium-copper oxide (Figs. 9 and 10). It was not physically possible to mount this grain in a polished section due to its small size. However, energy-dispersive spectrometer (EDS) analyses indicate average contents of 77.59% Pd, 17.08% As, and 5.33% Sb.

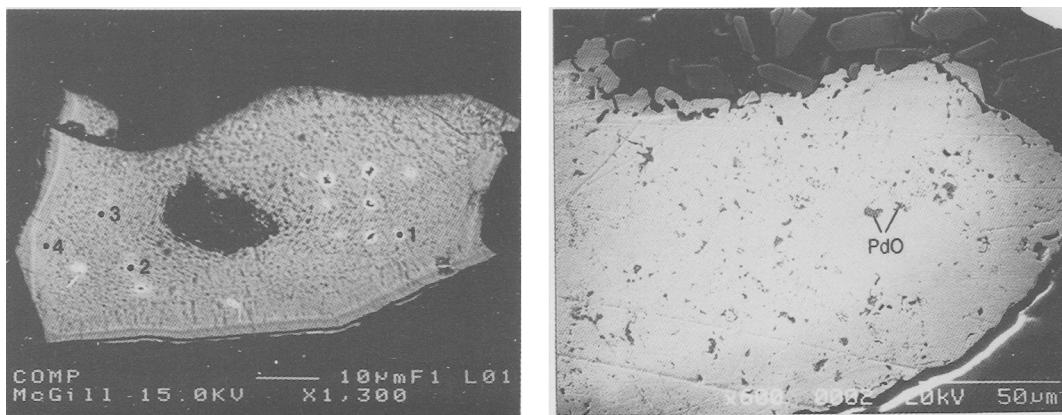
The occurrence of arsenopalladinite and palladseite in jacutinga raises the question about the genetic link between the palladium minerals in the gold washings previously described by Clark *et al.* (1974) and the palladium minerals found in the auriferous Cauê iron-formation. We suggest that jacutinga is the most probable source of these palladium minerals because: arsenopalladinite and palladseite, two of the four minerals described by Clark *et al.* (1974) were found in jacutinga; and the minerals described by these authors contain inclusions of palladium oxide and hematite which also occur in jacutinga.

Discussion

The palladium mineralization of the Corpo Y orebody in the Cauê iron mine was synchronous

TABLE 2. Wavelength-dispersive analyses by electron-microprobe of palladium-copper oxide from Jacutinga of Corpo Y orebody. Arabic numbers correspond to the analyses plotted in Figs. 5 (grain I), 6 (grain II) and 7 (grain III)

Grain	I				II				III				IV	V					
	1	2	3	4	1	2	3	4	5	6	7	8			9	1	2	3	4
PdO	95.81	90.30	90.38	87.88	93.60	90.37	89.45	90.76	93.30	88.06	89.07	88.72	88.69	91.51	89.71	87.67	88.90	87.87	91.51
CuO	4.51	5.47	7.06	6.74	7.40	7.41	8.04	7.78	7.37	8.40	8.40	8.03	7.76	7.25	7.51	6.87	7.58	8.27	7.93
HgO	0.46	0.05	1.05	1.20	0.82	0.67	0.91	0.80	1.21	1.42	1.35	0.56	0.36	1.56	1.57	1.48	1.55	1.34	1.49
AuO	0.53	0.35	0.47	0.14	0.07	0.10	n.d.	0.08	0.16	0.47	0.26	0.39	0.05	0.09	n.d.	n.d.	0.09	0.29	0.16
Fe ₂ O ₃	1.28	1.10	0.89	0.75	0.38	0.40	0.35	0.34	0.30	0.32	0.29	0.38	0.39	0.71	n.d.	0.77	0.60	0.25	0.34
SeO ₂	0.07	0.08	0.02	0.04	n.d.	0.04	0.03	0.01	n.d.	0.09	0.10	0.09	0.04	n.d.	n.d.	n.d.	n.d.	n.d.	n.d.
Sb ₂ O ₅	0.02	0.05	0.03	0.04	n.d.	0.01	n.d.	n.d.	n.d.	0.03	n.d.	0.03	0.01	n.d.	n.d.	n.d.	n.d.	n.d.	n.d.
Total	102.68	97.40	99.90	96.79	102.27	99.00	98.78	99.77	102.34	98.79	99.47	98.20	97.30	101.12	98.78	96.79	98.72	98.00	101.43
Pd	79.84	75.24	75.35	73.26	78.00	75.33	74.57	75.67	77.75	73.43	74.28	73.97	73.93	76.26	74.76	73.08	74.14	73.27	76.26
Cu	3.41	4.13	5.33	5.08	5.58	5.59	6.07	5.87	5.56	6.34	6.34	6.06	5.86	5.47	5.69	5.17	5.74	6.24	6.01
Hg	0.41	0.04	0.93	1.07	0.73	0.60	0.81	0.72	1.07	1.26	1.20	0.50	0.32	1.38	1.39	1.32	1.37	1.19	1.33
Au	0.47	0.32	0.60	0.12	0.06	0.09	n.d.	0.07	0.15	0.42	0.23	0.34	0.04	0.08	n.d.	n.d.	0.08	0.22	0.23
Fe	0.85	0.73	0.42	0.50	0.25	0.27	0.24	0.23	0.20	0.22	0.19	0.25	0.26	0.47	n.d.	0.51	0.40	0.19	0.14
Se	0.05	0.06	0.01	0.03	n.d.	0.03	0.02	0.01	n.d.	0.06	0.07	0.06	0.03	n.d.	n.d.	n.d.	0.51	n.d.	n.d.
Sb	0.01	0.03	0.02	0.03	n.d.	0.01	n.d.	n.d.	n.d.	0.02	n.d.	n.d.	0.01	n.d.	n.d.	n.d.	n.d.	n.d.	n.d.
Pd/Cu	23.41	18.21	14.13	14.42	13.97	13.47	12.29	12.89	13.96	11.58	11.71	12.21	12.61	13.94	11.13	14.13	12.92	11.74	12.69

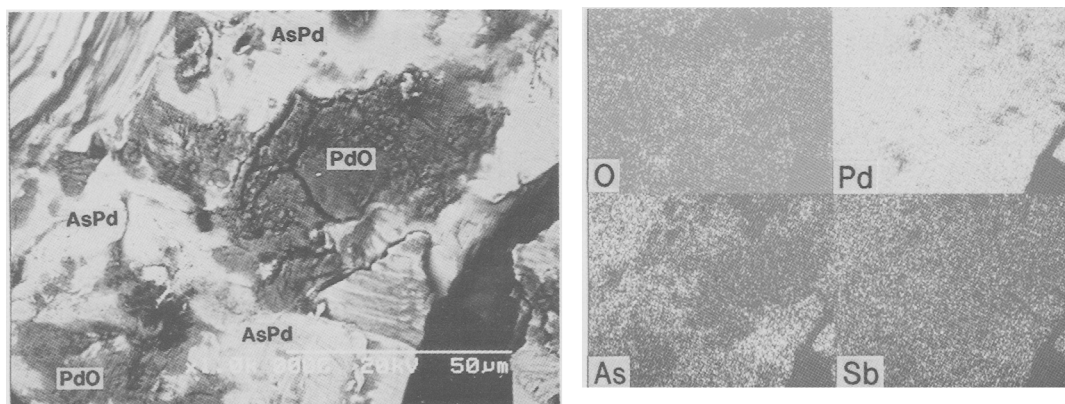


FIGS. 7 and 8. FIG. 7 (left). Back-scattered electron image showing a finely zoned palladium–copper-oxide grain (PdO) in a white phyllosilicate band parallel to the S1 mylonitic foliation. The oxide grain was coated with gold which was removed by repeated polishing, and contains fine inclusions of gold oblique to the compositional bands. Arabic numbers correspond to the analysed points referred to in Table 2. FIG. 8 (right). Back-scattered electron image of stretched gold with small inclusions of Pd-Cu oxides (PdO), showing island-mainland and replacement (relict) textures (from Corpo Y).

with the development of D1 structures. This interpretation is based on the presence of: (1) palladium copper oxide in hematite bands stretched parallel to the ENE elongation lineation in the plane of S1-mylonitic foliation; (2) palladium copper oxide and palladium grains in quartz and white phyllosilicate boudins parallel to the S1 mylonitic foliation; and (3) palladium copper oxide inclusions in gold strongly to weakly stretched parallel to the ENE elongation lineation.

The generation of the S1 mylonitic foliation was synchronous with the peak of thermal metamorphism

at about 600°C. This temperature is based on oxygen isotope studies in hematite and quartz (Hoefs *et al.*, 1982) and is in agreement with the metamorphic assemblages in the country rocks. The oxygen fugacities during the hydrothermal event, coeval with the peak of metamorphism, were as high as values equivalent to the hematite stability field; this finding is consistent with the hematitic composition of the iron-formation (itabirite, massive bodies of hematite, and jacutinga). Under these conditions, Pd and Au are favourably transported as chloride complexes (Henley, 1973; Seward, 1984; Mountain



FIGS. 9 and 10. FIG. 9 (left). Back-scattered electron image of arsenopalladinite (AsPd) with inclusions of palladium–copper oxide (PdO). FIG. 10 (right). Single-element scans of Pd, As, Sb and O for the area shown in Fig. 9.

and Wood, 1988; Gammons *et al.*, 1992). The deposition of these metals may have occurred in response to an increase in pH, resulting from mineralizing fluids reacting with the jacutinga, which, itself may be an altered dolomitic itabirite (Olivo *et al.*, 1994). A complementary mechanism of Pd deposition may have been the saturation of Pd with insoluble selenide and arsenide-antimonide (Mountain and Wood, 1988, Wilde *et al.*, 1989; Gammons *et al.*, 1992). This would explain the palladium grain with a palladseite core and the occurrence of arsenopalladinite in jacutinga.

The physico-chemical conditions may have oscillated during the D1 shearing event. This interpretation is based on: the presence of Pd-Cu oxide occurring as inclusions with replacement (relict) textures in gold grains stretched parallel to S1 foliation and as gold-coated grains (without replacement textures) stretched parallel to the S1 foliation and on the presence of zoned palladium and the other hydrothermal minerals (e.g. tourmaline and monazite).

The occurrence of gold, either with palladium inclusions showing replacement textures, or as coatings on palladium minerals, could be tentatively explained as follows. Gold probably replaced palladium minerals during the oxidation of a previous palladium phase in response to local changes in the physico-chemical conditions. If this occurred, the palladium, replaced by gold, may have precipitated as palladium copper oxide or palladium close to the site of replacement, and gold was probably deposited as a coating on the new palladium minerals. In Fig. 5, the gold coating around the stretched palladium oxide grain is wide in the pressure shadow regions, suggesting that the gold coating, as well as the palladium minerals, was deposited during the formation of the S1 mylonitic foliation.

The above features also suggest that palladium copper oxide formed during the shear-related hydrothermal mineralizing event and not by oxidation of earlier palladium minerals as result of weathering processes.

Conclusions

Palladium minerals in the jacutinga samples (palladium, palladseite and palladium copper oxide) are parallel to the S1 mylonitic foliation and/or the elongation lineation. They are commonly coated with films of gold and textural features suggested that they were deposited during the same deformational event. The S1 mylonitic foliation was synchronous with the peak of thermal metamorphism (approximately 600°C), and the oxygen fugacities during this event were as high as the hematite stability field. Under these conditions, palladium and gold are favourably

transported as chloride complexes. Deposition of these metals may have been prompted by an increase of pH due to mineralizing fluids reacting with jacutinga. The Pd may also have been deposited following saturation with insoluble selenide and arsenide-antimonides (as indicated by the presence of palladseite and arsenopalladinite).

Textural and compositional studies of palladium and other hydrothermal minerals suggest that oscillations in the physico-chemical conditions of hydrothermal fluids occurred during the mineralizing event. Finally, the occurrence of arsenopalladinite and palladseite in jacutinga suggests that this rock is the most probable source of palladium minerals found in residual concentrates from the gold washing at Itabira reported by Cabri *et al.* (1974).

Acknowledgements

G.R. Olivo gratefully acknowledges receipt of a Conselho Nacional de Desenvolvimento Científico e Regional (CNPQ, Brazil) graduate scholarship. Special thanks are extended to the geological staff and management of the Companhia Vale do Rio Doce (CVRD) in the Itabira and Belo Horizonte Districts for field work support and sample preparation and to M. Bardoux for stimulating discussions on structural data. We are also grateful to Glenn Porrier (McGill) and Raymond Mineau (UQAM) for assistance during EMP and SEM analyses, respectively, to C.L. Jenkins for improving the English, and to M. Laithier for drafting the figures. This work was partly supported by FCAR funding from the Quebec Government. We thank the Mineralogical Magazine reviewers for their constructive criticism on an earlier draft of the manuscript.

References

- Cabri, L.J., Clark, A.M., and Chen, T.T. (1977) Arsenopalladinite from Itabira, Brazil, and from the Stillwater Complex, Montana. *Canad. Mineral.*, **15**, 70–73.
- Clark, A.M., Criddle, A.J. and Fejer, E.E. (1974). Palladium arsenide-antimonides from Itabira, Minas Gerais, Brazil. *Mineral. Mag.*, **39**, 528–43.
- Davis, R.J., Clark, A.M. and Criddle, A.J. (1977). Palladseite, a new mineral from Itabira, Minas Gerais, Brazil. *Mineral. Mag.*, **41**, 123.
- Gammons, C.H., Bloom, M.S. and Yu, Y. (1992) Experimental investigations of the hydrothermal geochemistry of platinum and palladium: I. Solubility of platinum and palladium sulfide minerals in NaCl/H₂SO₄ solutions at 300°C. *Geochim. Cosmochim. Acta*, **56**, 3881–94.
- Henley, R.W. (1973) Solubility of gold in hydrothermal chloride solutions. *Chem. Geol.*, **11**, 73–87.

- Hoefs, J., Muller, G. and Schuster, A.K. (1982) Polymetamorphic relations in iron ores from Iron Quadrangle, Brazil: the correlation of oxygen isotope variations with deformation history. *Contrib. Mineral. Petrol.*, **79**, 241–51.
- Ineson, P.R. (1989) *Introduction to practical ore microscopy*. Longman Earth Science Series, John Wiley & Sons, Inc., New York, 181 pp.
- Jedwab, J., Cassedanne, J., Criddle, A.J., Ry P., Ghysens, G., Meisser, N., Piret, P. and Stanley, C.J. (1993) Rediscovery of palladinite PdO from Itabira (Minas Gerais, Brazil) and from Ruwe (Shaba, Zaire). *Abstract Supplement no. 3, Terra Nova*, **5**, p. 21.
- Leao de Sá, E. and Borges, N.R.A. (1991) *Gold mineralization in Cauê and Conceição iron ore mines, Itabira-MG. Field guide book of Brazil Gold'91: An international symposium on the geology of gold.* (Fleisher, R., Grossi Sad, J.H., Fuzikawa, K., Ladeira, E. A, eds), pp. 74–85.
- Mountain, B.W. and Wood, S.A. (1988) Chemical controls on the solubility, transport, and deposition of platinum and palladium in hydrothermal solutions: a thermodynamic approach. *Econ. Geol.*, **83**, 492–510.
- Olivo, G.R., Gauthier, M. and Bardoux, M. (1994) Palladian gold from the Cauê iron mine, Itabira District, Minas Gerais, Brazil. *Mineral. Mag.*, **58**, pp. 579–87.
- Olivo, G.R., Gauthier, M., Bardoux, M., Leao de Sá, E., Fonseca, J.T.F., Santana, F.C. (1995) Palladium-bearing gold deposit hosted by Proterozoic Lake Superior-type iron-formation at Cauê iron mine, Itabira district, Southern Sao Francisco Craton, Brazil: geologic and structural controls. *Econ. Geol.*, **90**, 118–34.
- Seward, T.M. (1984) The transport and deposition of gold in hydrothermal systems. In *Proceedings of the Symposium Gold'82: the geology, geochemistry and genesis of gold deposits* (Foster, R.P., ed.). A. A. Balkema, Rotterdam, pp. 165–81.
- Wilde, A.R., Bloom, A.S. and Wall, V.J. (1989) Transport and deposition of gold, uranium and platinum-group elements in unconformity-related uranium deposits. *Econ. Geol. Monogr.* **6**, 637–60.

[Manuscript received 14 July 1994:
revised 4 October 1994]